Published in final edited form as:
*J Mol Biol*. 2010 May 14; 398(4): 584–599. doi:10.1016/j.jmb.2010.03.017.

# Key amino acid residues involved in multi-point binding interactions between brazzein, a sweet protein, and the T1R2-T1R3 human sweet receptor

**Fariba M. Assadi-Porter**[a,§,*], **Emeline L. Maillet**[b,§], **James T. Radek**[a], **Jeniffer Quijada**[b], **John L. Markley**[a], and **Marianna Max**[b,c]

[a] National Magnetic Resonance Facility at Madison, Biochemistry Department, University of Wisconsin-Madison, 433 Babcock Drive, Madison WI 53706, USA

[b] Department of Neuroscience, Mount Sinai School of Medicine, 1425 Madison Ave, box 1065, New York, NY 10029, USA

[c] Department of Physiology and Biophysics, Mount Sinai School of Medicine, 1 Gustave Levy Place, New York, NY 10029, USA

## Abstract

The sweet protein brazzein activates the human sweet receptor, a heterodimeric G-protein coupled receptor (GPCR) composed of subunits T1R2 and T1R3. In order to elucidate the key amino acid(s) responsible for this interaction, we mutated residues in brazzein and each of the two subunits of the receptor. The effects of brazzein mutations were assayed by a human taste panel and by an *in vitro* assay involving receptor subunits expressed recombinantly in human embryonic kidney cells; the effects of the receptor mutations were assayed by the *in vitro* assay. We mutated surface residues of brazzein at three putative interaction sites: Site 1 (Loop43), Site 2 (N- and C-terminus and adjacent Glu36, Loop33), and Site 3 (Loop9–19). Basic residues in Site 1 and acidic residues in Site 2 were essential for positive responses from each assay. Mutation of Y39A (Site 1) greatly reduced positive responses. A bulky side chain at position 54 (Site 2), rather than a side chain with hydrogen bonding potential, was required for positive responses as was the presence of the native disulfide bond in Loop 9–19 (Site 3). Results from mutagenesis and chimeras of the receptor indicated that brazzein interacts with both T1R2 and T1R3 and that the Venus fly trap module of T1R2 is important for brazzein agonism. With one exception, all mutations of receptor residues at putative interaction sites predicted by wedge models failed to yield the expected decrease in the brazzein response. The exception, hT1R2:R217A-hT1R3, which contained a substitution in lobe 2 at the interface between the two subunits, exhibited a small selective decrease in brazzein activity. However, because the mutation was found to increase the positive cooperativity of binding by multiple ligands proposed to bind both T1R subunits (brazzein, monellin, and sucralose) but not those that bind to a single subunit (neotame and cyclamate), we suggest that this site in involved in subunit-subunit interaction rather than direct brazzein binding. Results from this study support a multipoint interaction between brazzein and the sweet receptor by some mechanism other than the proposed wedge models.

[*]To whom correspondence should be addressed, National Magnetic Resonance Facility at Madison, Biochemistry Department, University of Wisconsin-Madison, 433 Babcock Drive, Madison WI 53706, USA. Phone: 608-261-1167; Fax: 608-262-3754; fariba@nmrfam.wisc.edu.
[§]These authors contributed equally to the studies presented in this manuscript.

**Keywords**

Brazzein; sweet protein; heterodimeric sweet receptor; calcium assay; psychophysical assay; G-protein coupled receptor

# INTRODUCTION

## Sweet tasting compounds

A wide variety of chemically diverse compounds taste sweet, including natural sugars, such as glucose, fructose, sucrose, and sugar alcohols. Non-carbohydrate sweet-tasting substances include several chemically distinct groups of small molecule artificial sweeteners, such as sucralose, saccharin, cyclamate, and acesulfame K, as well as dipeptide sweeteners, such as aspartame and neotame. Sweet-tasting proteins have been found as naturally occurring molecules from plants (or rarely from animals) including thaumatin [1], monellin [2], mabinlin [3], brazzein [4; 5], eggwhite lysozyme [6], and curculin/neoculin [7]. In addition, a pure sweet-antagonist protein, the glycoprotein RBP from chicken egg, has been reported to inhibit specifically the taste of sweet-protein but not carbohydrates or artificial sweeteners [8]

## Brazzein

Brazzein is the smallest known protein with a sugar-like taste. The protein is found naturally in berries of the African plant *Pentadiplandra brazzeana*. The molecule is 17,000 times sweeter than sucrose on a molar basis. Brazzein is sweet only to humans and old world monkey species [9], whereas rodents and new world monkey species are indifferent to brazzein. Brazzein has been successfully produced heterologously in bacterial expression systems [10; 11]. The three-dimensional structure of brazzein isolated directly from fruit was determined by NMR spectroscopy [12]. Brazzein, which belongs to the Csβα fold family, contains three anti-parallel $\beta$-strands and a small $\alpha$-helix (Fig. 1A). Strand I is followed by a stretch of flexible residues in Loop9–19. The cysteine at position 16 connects this loop to the cysteine at position 37 in the middle of strand II. Loop9–19 is followed by the $\alpha$-helix, the short Loop-33, and the remaining two strands of $\beta$-sheet (strands II and III). Strands II and III are connected by a short, 3–4 residue loop (the Arg43 Loop). The three $\beta$–strands are connected by backbone hydrogen bonds and a web of disulfide bonds that maintain the structure in a stable conformation.

## The sweet receptor

The sweet receptor consists of a heterodimer of two sequence-related subunits that belong to the class C GPCR family: Taste type 1 Receptor 2 (T1R2) and 3 (T1R3) [13] (Fig. 1B). On the basis of their sequence similarities to mGluR1, 3 & 7 and rhodopsin [14; 15; 16], each subunit has been proposed to consist of three main structural domains: the Venus flytrap module (VFTM) containing lobes 1 and 2, which can be in an “open” or “closed” conformation, the cysteine-rich domain (CRD) named for 9 conserved cysteine residues in the mGluR subgroup of Family C, and the heptahelical transmembrane domain (TMD) [17] (Fig. 1B). The CRD links the VFTM and the TMD. In the closed conformation, a binding cavity is formed between the bottom of lobe 1 and the top of lobe 2 of each VFTM. In T1R2, this cavity has been proposed to be the orthosteric binding site for naturally occurring sweet carbohydrates and the binding site for dipeptidic artificial sweeteners like aspartame and neotame [18]. These two lobes are joined at the back of the binding cavity by three sequentially discontinuous beta strands that form a hinge that flexes between the open and closed states of the VFTM. Within the dimeric family C receptors, receptor activation appears to involve closure of the VFTM domain of at least one subunit and mutual rotation of the subunits around their dimerization contact domain [19]. Homology-based structural models of the open and closed forms of the VFTMs from the

sweet receptor [20; 21; 22; 23] have been derived from crystal structures of other class C GPCRs [14; 15; 24].

## Sweet protein/sweet receptor interactions

Although sweet proteins display low sequence and structural similarity to one another, it has been proposed that they might share a common mechanism for receptor activation [25]. Various "wedge" models [23; 25; 26; 27; 28] postulate that sweet proteins, such as brazzein, monellin, and thaumatin, and sweet-modifying glycoproteins, such as miraculin [29] and curculin [30], dock in the open cleft of either T1R2 or T1R3 despite their large size relative to the dimensions of the cleft [31; 32] (Fig. 2). Neoculin's dual sweetness and sweet-modifying properties have been shown to map to partially overlapping, but distinct, molecular surfaces [30]. Interestingly, the hT1R3 VFTM appears to be essential for the activity of neoculin [33], and *in silico* docking studies suggested that it binds in the T1R3 cleft [22].

## Brazzein mutations that alter sweetness

The major sites of brazzein's interactions with the sweet receptor, based on mutagenesis studies, were proposed to be Loop43 (Site 1) and the N- and C-terminal regions (Site 2) (Fig. 1A) [10]. In addition, nearby Loop33 and Loop9–19 (Site 3) make significant contributions to brazzein's sweetness. Ala-scanning studies aimed at elucidating the physicochemical basis of brazzein's sweetness [34; 35; 36] demonstrated the importance of charged Arg and Lys residues in the loop regions. Mutation R43A (Site 1) resulted in profoundly reduced activity [34]. Mutations R33A (Loop33, Site 2) and Q17A (Loop9–19, Site 3) led to smaller, but significant, reductions in sweetness. Substitutions D29K, D29N, D29A [35], or H31A [34] increased sweetness. In contrast, substitutions in Loop9–19 reduced sweetness by factors of 2–4 [34]. Substitutions of residue E36 (which lies near the C-terminus in the 3D structure – Site 2) by A, Q, or K significantly reduced sweetness [34; 35; 36]. Deletion of Y54 (the C-terminal residue – Site 2) or insertions of two amino acids at the C-terminus (Site 2) completely eliminated sweetness, indicating that the length of the C-terminus is important for brazzein's sweetness and suggesting that the C-terminus may interact directly with the sweet receptor [34]. Because the residues required for brazzein sweetness are distributed widely on the surface of the protein, a multi–binding–site interaction model for brazzein to the sweet receptor was proposed [34].

In a previous study, we showed that the heterologously-expressed human sweet receptor is responsive to sweet proteins but that the mouse T1R2-T1R3 receptor is completely unresponsive to them [37]. We also showed that an interspecies receptor composed of human T1R2 and mouse T1R3 was partially responsive to monellin but unresponsive to brazzein. We went on to show that specific residues of the CRD of T1R3 must be of the human form for the chimeric or mutant receptors to be responsive to brazzein. However, at that time we could not assess the contribution of the human T1R2 subunit because of incompatibility between the mouse T1R2 and the human T1R3 subunits. The present study was designed to determine whether residues in T1R2 also contribute to brazzein's activity.

## Current studies

In order to better understand the molecular determinants of brazzein's sweetness, we made additional mutations in all three putative interaction sites and evaluated their effects both by human psychophysical tests of brazzein's sweetness, and by a cell-based functional heterologous-expression assay that measured sweet receptor-stimulated (T1R2 + T1R3) calcium mobilization in response to brazzein or other sweeteners. The *in vitro* assay also enabled us to evaluate published models for brazzein-sweet receptor interaction [23; 25; 28] by making and testing a series of T1R2-T1R3 receptor mutants. These included an interspecies T1R2 chimera and point mutations of T1R2 and T1R3 that were designed to determine the

involvement of the extracellular domains (VFTMs) of the sweet receptor in brazzein sensitivity.

# RESULTS

## Assays for brazzein sweetness

As in our earlier human taste studies, we used a stepwise scale to determine the observed threshold concentration and to measure brazzein sweetness above threshold [34]; we also compared variants at a single concentration [38;35]. Studies involving human taste panels are subject to background genetic variations and subjective differences in perception; therefore, in addition to the human taste panel assay, we used a calcium-mobilization cell-based assay, with heterologously expressed human sweet taste receptors, to assess the sweetness of brazzein and its mutants. Human sweet receptor (T1R2 + T1R3) was expressed in human embryonic kidney cells together with the G-protein reporter chimera, G16gus44, which mobilizes calcium from internal stores upon activation of sweet receptors [39]. As shown in Figure 3, this system produced a specific and robust calcium signal ($\Delta F/F$, see methods) in response to a diverse panel of sweeteners (e.g., neotame, cyclamate, *N*-saccharin, sucralose, D-tryptophan, sucrose, and brazzein).

## Results with brazzein mutations

A total of 21 brazzein mutants were made for this study (Table 1). They were chosen to assess the roles of surface exposed amino acids in Sites 1–3. A three-dimensional representation of the protein surface from a high-resolution (RMSD = 0.38 Å) NMR structure of recombinant wild-type brazzein (C. C. Cornilescu, F. M. Assadi-Porter, et al., manuscript in prep.), provides a visual summary of the taste properties of these variants in the context of those previously reported [34; 35; 36] (Fig. 4). Mutations that led to increased sweetness are indicated in red; those that reduced sweetness are in light blue; and those that abolished sweetness are in dark blue.

A pychophysical analysis (taste panel) of wild type brazzein (WT) and a series of brazzein mutants was obtained and averaged from 10 subjects (Fig. 5A). The human taste panel compared the sweetness of 100 μg/ml solution of brazzein to that of a 2% solution of sucrose to obtain a sweetness score. The cell-based calcium mobilization assay (Fig. 5B) evaluated the relative potency of each variant in comparison to wild type brazzein over a range of four concentrations (100, 30, 10, 3 μg/ml). The maximal response of the receptors in each experiment was quantified using a saturation concentration of the agonist neotame (50μM), and data were normalized to 100 % of this value. In general, both assays reported nearly identical levels of sweetness/activity relative to wild type for each mutant brazzein; thus the results are presented below in tandem for brevity.

### Site 1

Results with **E41A** confirmed earlier findings [35] that removal of the negative charge at Glu41 increases sweetness and responsiveness. Additionally, Ala replacements at Tyr39 (**Y39A**) (non-sweet mutant) and Lys42 (**K42A**) each decreased sweetness in both assays. Mutations that reversed, neutralized, or swapped charge in Site 1 residues, **D40K, E41Q**, and **E41K/K42E**, increased the sweetness significantly from that of wild type brazzein. **D40K** (negative to positively charged side chain) was perceived to be the sweetest variant of this group.

Mutations **R43E** (positive to negatively charged residue) and **R43N** (positive to polar uncharged residue) made brazzein much less sweet. **R43K,** a mutation that changes the size of the side chain but preserves the charge, rendered the resulting mutant brazzein moderately less sweet. This suggests that this site has very specific charge and size constraints and that only Arg at this position allows brazzein to maintain full sweetness.

### Site 2

Previously we showed that the C-terminal residue, Tyr54 cannot be truncated without loss of sweetness [34]. Here we show that sweetness is retained when Tyr54 is substituted by another residue containing a bulky side chain. **Y54H** showed a small loss and **Y54W** a small gain in sweetness in both the in vivo and in vitro assays. Thus bulkiness, rather than specific chemical interactions, is required at this position in Site 2.

The N-terminus of brazzein (part of Site 2) has been shown to play a role in sweetness. The N-terminal insertion mutations, **D2insII** and **D2insGP** (insertions of two hydrophobic residues) both increased sweetness. We showed previously that **D2N** and **K5A** replacements resulted in decreased sweetness [34]. Here we show that increasing the size of the side chains (**D2E** or **K5R**) while maintaining the charge leads to little or no change in sweetness; thus, we conclude that the charges at these positions are essential to function.

In a prior study, we determined that the C-terminal mutation D50A decreased sweetness [34]. The present results show that replacement of the negative charge at this position by a polar side group, **D50N,** actually increased sweetness in both the in vivo and in vitro assays; thus, a negative charge is not required at this position.

### Site 3

Mutations that alter the disulfide bond in Site 3 render brazzein non-sweet. The non-sweet mutants are **C16A/C37A**, which abolishes the C16–C37 disulfide bridge, **C16A/Q17C**, which moves the position of this disulfide bridge, and **C16A/C37A/**L18_A19insRI, which removes the disulfide bridge and increases the size of Loop9–19.

We used $^{15}$N-HSQC NMR spectroscopy to evaluate the overall fold of mutants. The spectra (Fig. 6) showed that the $^{1}$H-$^{15}$N cross peaks are dispersed as indicative of folded protein; however, widespread chemical shift differences from wild type brazzein suggested that these mutants have altered conformations. Large changes were observed in the chemical shifts of residues near the N- and C- termini, as well as smaller chemical shift changes in the $\alpha$-helix and in residues of Loop 33. Thus, altered disulfide formation in Site 3 causes perturbations of residues in Sites 1 and 2, and these changes may explain the loss of sweetness. The C17–C37 disulfide of mutant **C16A/Q17C** was determined to be oxidized on the basis of the $^{13}C^{\beta}$ chemical shifts of Cys17 and Cys37 observed by HNCACB NMR spectroscopy [40].

### Sweet receptor variants

The sweet receptor variants studied are summarized in Table 2 and Figures 7, 8. These variants, which include functional receptors composed of a “humanized” mouse T1R3 subunit (mT1R3:T542A/P545F) and a chimeric mouse/human T1R2 subunit (Fig. 7A, B), were designed to test whether human specific residues in the VFTM and CRD extracellular domains of T1R2 are required for the brazzein response. In contrast to results with other sweeteners, such as sucralose, we found that when hT1R2 is paired with mT1R3:T542A/P545F, the brazzein response is about twice that when mouse T1R2 is paired with mT1R3:T542A/P545F (in Fig. 7B, compare the effect of brazzein vs. sucralose with m-R2+mAF-R3 to that with hm1&2-R2 + mAF-R3). Brazzein responses with the human-mouse T1R2 chimeras were proportionally similar to that with fully human T1R2, when the chimera contained both hVFTM and hCRD (mT1R2:hVFTM/hCRD) or when the chimera contained only hVFTM (mT1R2:hVFTM) (Fig. 7B). These results indicate that brazzein is more active when human specific residues in the VFTM of T1R2 are present, although this effect is modest. Our results do not rule out a role for the VFTM of T1R2 in the response to brazzein, although they do underscore our previous finding that it is human residues in the CRD of T1R3 that are critical for the species-specific response to brazzein.

To explore the involvement of residues predicted by "wedge-models" for brazzein-receptor interaction, we mutated VFTM residues in both T1R2 and T1R3 (Fig. 2 and methods section). As shown in Figure 8A,B, the range of concentrations tested permitted the detection of specific changes in sensitivity to neotame or cyclamate for mutants T1R2-S144A and T1R3-F730L respectively, in agreement with previously published results [20; 41]. Sucralose (a VFTM-T1R2 and VFTM-T1R3 agonist) was used at saturating concentration ($25\times EC_{50}$) in order to compare the maximal response ($E_{max}$-sucralose) between WT and mutant receptors. Results of the mutational screening are shown in Figure 8C (T1R2-VFTM model) and Figure 8D (T1R3-VFTM model).

Some mutant receptors (T1R2:D173A/R, Y215A, R217D, and T1R3:E172R, Y218A/R) failed to respond to any tested sweetener (0–10% versus WT); this result ruled out investigation of the potential role of these residues in specific brazzein interaction (Fig. 8C,D, Sup. Fig 1). Mutants that exhibited proportional changes across the panel of sweeteners served to identify residues involved in global receptor responses, rather than residues involved in a specific interaction with brazzein (Fig. 8C,D, Sup. Fig 1). Among the residues predicted by wedge models to interact with brazzein that were mutated, only T1R2:R217A showed a proportionally lower response to the threshold concentration of brazzein than to other sweeteners in the panel (Fig. 8D, Sup. Fig 1). However, when we determine the full dose-responses curves to these sweeteners (neotame, cyclamate, sucralose, brazzein, and monellin; Fig. 9, Sup. Fig. 2), we found that the change was proportional for all sweeteners. The global responsiveness of this receptor mutant was half that of WT for all sweeteners tested (Sup. Fig. 1), and the full dose response curve revealed that the half-maximal activity for brazzein and the other sweeteners was only slightly modified (Fig 9A, B, Sup Fig. 2). Interestingly, the slopes of the saturation curves ($n_{Hill}$) for brazzein, monellin, and sucralose were higher with the T1R2:R217A mutant than with WT receptor (Fig. 9A,B), a result suggesting that this mutation increases the cooperativity for receptor activation by these three sweeteners.

## DISCUSSION

With the exception of the disulfide mutations and insertions, all brazzein mutations investigated here were limited to surface residues not involved in intramolecular interactions. Hence, the mutations were not expected to lead to major structural changes, and the results can be interpreted in terms of receptor interactions. In our earlier work, we discovered that multiple, distributed sites are important for brazzein's sweetness. Two arginines (R33 and R43) were shown to be important for brazzein's sweetness [34]. Mutant R43A was shown to exhibit profoundly reduced sweetness (only slightly sweet in powder form) [34; 42]. R43 is part of the critical Site 1 loop (Loop43) further investigated here by mutagenesis, biochemical studies, and human taste trials. Our previous investigations of R43A [43] showed that, although the structure of the mutant resembles that of wild type, it is more rigid. Other mutants that exhibited reduced internal dynamics also had reduced sweetness [41]. These results have suggested that dynamics may play an important role in brazzein's interaction with the sweet receptor.

The Site 1 mutants prepared for this study evaluated the Loop43 region (Y39A, D40K, E41A/Q, E41K/K42E, K42A, and R43K/E/N). These new mutations exhibited a variety of potencies: some were less sweet and some sweeter than wild type brazzein. It is clear from these studies that mutations that reduce the overall negative charge at this site and/or increase or preserve the positive charge (D40K, E41A/Q, E41K/K42E) favor brazzein potency. Mutations that reduce the positive charge at this site, even while preserving polar moieties, reduced (K42E) or abolished (R43E/N) sweetness. These results suggest that Site 1 contributes a dipole that is important for brazzein sweetness; however, the loss of brazzein potency by mutant R43K indicates that the size of this residue and potentially a specific binding contact with the receptor are also important features of brazzein activity. The requirement for a positively charged side

chain of a particular size at position 43 suggests that there might be a corresponding negatively charged surface of interaction on the receptor that forms a salt bridge.

We previously showed that alanine scanning mutants that removed positive charge at specific residues near the N terminus (K3A, K5A, K6A) or C-terminus (R33A) (in Site 2) reduce brazzein's sweetness [34]. Here we report that mutants D2E and K5R retain sweetness, a result indicating that the charge of the residue, rather than its size, is critical. Mutant D50N, which removes negative charge in the C-terminal segment of Site 2, increased sweetness. As in Site 1, negatively charged residues in WT brazzein may limit brazzein's overall sweetness or its temporal sensory properties. Because substitution of E36 (Site 2) by A, K, or D resulted in significant losses of sweetness, this residue may be involved in a more specific type of interaction with the receptor, perhaps by formation of a hydrogen bond or salt bridge.

The roles of aromatic side-chains in Sites 1 and 2 were investigated by their deletion or conversion to Ala or a bulky residue. Deletion of Y54 completely abolished the sweetness of brazzein [34]. However, since mutation of Y54 to tryptophan or histidine led to no significant change of sweetness, the presence of a bulky residue at position 54, rather than its chemical nature, appears to be important for its interaction with the receptor. When the solvent exposed residue Y39 was mutated to alanine, it resulted in a tasteless brazzein. This residue may be involved in receptor binding through either a π-π or hydrophobic interaction as previously proposed [34; 44]. Our results support the existence of a network of electrostatic, π-π, H-bonding, and steric interactions between brazzein and the receptor over a multi-point interaction surface.

In the current study, we explored the size and position of the disulfide bond located in Loop19 (Site 3). Mutations that removed the disulfide (C16A/C37A), moved the disulfide (C16A/Q17C), increased the size of the loop (RI-insertion), or removed the disulfide and increased the loop size (C16A/C37A/L18_A19insRI) all abolished sweetness. NMR studies indicated that each of these mutations led to large conformational changes throughout the protein.

Although progress has been made in elucidating the roles of key residues of sweet and sweet-modifying proteins in relation to their agonistic and pH-sensitive interactions with the sweet receptor, a detailed model for the interaction between brazzein and other sweet proteins and the sweet receptor remains to be determined. The early "sweet-finger" model [31] for the sweet protein-receptor interaction was invalidated by experiments. First, peptides designed to contain sweet fingers failed to be sweet [45], and, second, point mutations of the receptor at proposed contact sites failed to block responses triggered by sweet proteins [32]. Subsequent "wedge" models [23; 25; 27; 28], derived by homology modeling from the X-ray structure of the homodimeric mGlu receptor, showed brazzein or other sweet proteins docked into the open clefts of T1R2 or T1R3. The wedge-models describe a potential new mechanism in which brazzein (or other sweet proteins) bind within the cleft/mouth of the open form of VFTM-T1R2 (Fig. 2A) and/or within the cleft/mouth of VFTM-T1R3 (Fig. 2B).

We demonstrated here that the response to brazzein of the human form of T1R2 VFTM is about twice that of the mouse form. This is consistent with the previous finding that monellin requires human-specific residues in the T1R2 VFTM for its function [37]. This is also consistent with the notion that the VFTM of T1R2 may be part of the binding site for protein sweeteners. This leaves open the question of whether wedge models that position brazzein within and adjacent to the cleft within the VFTM of T1R2 can explain protein sweetener activities. To test such wedge models, we mutated receptor residues predicted to contact brazzein (Fig. 2) and tested their effect by means of the functional assay (Sup. Fig. 1 and Fig. 8). However, none of the mutations tested produced the expected brazzein-specific decrease in the response of the assay to the panel of sweeteners.

We previously reported that specific residues in the extracellular cysteine rich domain (CRD) of T1R3 are important for brazzein's agonisticity [37]. We further found by saturation transfer difference NMR spectroscopy that membranes derived from HEK cells expressing WT hT1R2 + hT1R3:D535Q, a CRD-mutant of T1R3 with a "brazzein-specific activation deficit", exhibited decreased binding to the receptor compared to membranes from HEK cells expressing WT hT1R2 + WT hT1R3 [46]. These findings confirm the importance of brazzein's interaction with the CRD of hT1R3 to receptor activation.

In the calcium flux assays reported here, receptor mutant T1R2:R217A exhibited higher cooperativity than WT to sweet proteins and sucralose (but not other sweeteners in the test panel). Our homology model for the sweet receptor shows T1R2:R217 lying in lobe 2 facing into the space that separates the VFTMs of T1R2 and T1R3. What do protein sweeteners and sucralose have in common that they would be similarly affected by the R217 mutation? As we have demonstrated here, the activity of protein sweeteners depend on residues in both subunits. Interestingly, sucralose and other natural sweeteners have been shown to bind the VFTM of T1R2 and to a lesser extent the VFTM of T1R3 [47], whereas neotame binds only T1R2-VFTM. This suggests that R217 helps to govern coordinated conformational changes between subunits when they are simultaneously bound by full agonists. It is interesting to note that R217 is homologous to one of the 'negative patch' residues that controls allosteric interactions in the metabotropic glutamate receptor [48]. Further study of this position and its homologous R220 residue in T1R3 may shed light on the interesting question of allosteric interaction between VFTMs on the two subunits.

Our current data do not rule out direct contact between brazzein and T1R2-VFTM; in fact, our finding of a two-fold higher brazzein response by the human (compared to mouse) form of T1R2-VFTM is consistent with such an interaction. None of the receptor mutations designed to test the "wedge models", yielded results consistent with such models. Thus, it seems unlikely that brazzein binds directly into the open cleft of T1R2 or T1R3 as postulated by the wedge models. The wedge models also are inconsistent with structural studies of other class C GPCRs showing that a closed cleft conformation is required for binding [14; 15; 50]. Moreover, examination of the probable arrangement of the two VFTMs and the CRD of T1R3 reveals that the distance between these three domains is too great for brazzein to span. Alternatively, it could be proposed that brazzein activates the receptor in a series of multiple-step binding events per T1R2/T1R3 pair. However, there is currently no support for such a complex activation scheme. The data presented here provide useful constraints for future modeling and prediction of sweet protein-sweet receptor interactions.

## MATERIALS AND METHODS

### Mutagenesis and protein expression of brazzein

The synthetic gene for wild-type brazzein gene (the variant that lacks an N-terminal pGlu1 and has Asp2 as the N-terminus) in the nuclease fusion construct [10] was used as the template for specific amino acid substitutions. In the current study, a $His_6$ tag was inserted at the N-terminus of the fusion sequence to aid in purification of the fusion protein. Brazzein mutants were constructed by site directed mutagenesis (Quick Change™ PCR kit, Stratagene, La Jolla, CA) as described earlier [10]. Cells were induced at 3 h by addition of IPTG to a final concentration of 0.1 mM. The fusion protein was solubilized from inclusion bodies in 6 M GdmCl containing 10 mM EDTA and 100 mM DTT [10]. The protein isolated from inclusion bodies was refolded by dilution into a buffer lacking GdmCl and DTT, which led to formation of the four disulfide bridges. Brazzein was then separated from the fusion protein by CNBr cleavage at an engineered methionine and purified by $Ni^+$-NTA column chromatography. Refolding and product purity were checked by reversed-phase HPLC [10], MALDI mass spectrometry, and $^1$H-NMR spectroscopy [10] as previously described (data not shown). The extinction

coefficient $\varepsilon_{205}$ of each brazzein variant was calculated from measurements of the absorbance of solutions at 280 nm and at 205 nm according to the formula [49]: $\varepsilon_{205}{}^{1\ mg/ml} = 27.0 + 120 \times (A_{280}/A_{205})$. Mutant brazzein concentrations were determined from the absorbance at 205 nm.

## Human taste panel

A human taste panel evaluated the wild type and mutant proteins (according to an approved human subjects protocol). This panel, which was experienced in evaluating the taste properties of brazzein mutants, compared solutions of the mutants with those of wild-type brazzein and sucrose [35]. The 9-member panel included both sexes and represented different age groups. 150 μl aliquots were delivered to the tip of the tongue by pipette. After each taste trial, the subjects spit out the solution and rinsed their mouths with tap water for one minute. The concentration of the protein samples varied between 25–200 μg/ml. To score taste sensation, we used the Magnitude Labeled scale [38]: strongest imaginable, very strong, strong, moderate, weak, and barely detectable. After the taste trials, the qualitative scale was transformed into a numerical scale. The experimental data from different subjects were averaged using analysis of variance (ANOVA).

## NMR data collection

All NMR spectra were collected at the National Magnetic Resonance Facility at Madison (NMRFAM) on INOVA 600 MHz Varian instruments. Spectrometers used for data collection were equipped with single *z*-axis HCN gradient cryogenic probes. All NMR spectra were recorded at 37 °C. Two-dimensional (2D) $^{15}$N-$^{1}$H HSQC data sets were collected from [U-$^{15}$N]-variants to screen for chemical shift changes relative to wild-type brazzein in the amide “fingerprint” region. Two-dimensional $^{1}$H-$^{15}$N HSQC data were collected using a sensitivity-enhanced pulse sequence with 64–128 accumulations for each increment. NMR data were processed using NMRPipe (http://spin.niddk.nih.gov/bax/software/NMRPipe) and analyzed using Sparky (http://www.cgl.ucsf.edu/home/sparky). All spectra were zero filled once in the direct dimension, while the indirect dimension of 2D spectra was zero filled twice and apodized using sine square functions occasionally combined with Gaussian functions to enhance peak resolution.

## Small molecule tastants

Cyclamate, D-tryptophan, saccharin and sucrose were purchased from Sigma. Sucralose was from McNeil Specialty (New Brunswick, NJ). Neotame was a gift from the NutraSweet Company. Solutions were prepared on the day of the experiment. Powders were dissolved in HBSS buffer (Invitrogen, Carlsbad, CA) supplemented with 20 mM HEPES.

## Design of brazzein mutants

The brazzein mutants were designed to test the roles of various residues in the three putative receptor interaction sites (Fig. 1A).

**Site 1—Y39A**, **E41A**, and **K42A** probe the roles of these side chains; **R43K** changes the size of the side chain while preserving the positive charge; **D40K**, **R43E**, and **E41K/K42E** reverses or swaps the charge; **E41Q** and **R43N** neutralize the charge while roughly maintaining the size of the side chain.

**Site 2—**Mutations **D2insII** and **D2insGP** insert two extra amino acids before the native N-terminal residue D2. Mutations **D2E, K5R**, **Y54H**, and **Y54W** change the sizes of side chains while preserving their chemical nature (charge or ring); **D50N** removes a negative charge while preserving the size of the side chain.

**Site 3—**Double mutant **C16A/C37A** removes the disulfide bridge between Loop 19 and the connecting β-strand II, and double mutant **C16A/Q17C** moves the position of this disulfide bridge. Insertion of two residues in Loop 9–19 (L18_A19insRI) serves to probe the importance of the size of this loop.

### Sweet receptor chimera and point mutations

Point mutations in human VFTM of T1R2 and T1R3 receptors were made by site-directed mutagenesis according to manufacturer protocol (Quick Change™ PCR kit, Stratagene, La Jolla, CA). The chimera were prepared by overlapping PCR. The integrity of all DNA constructs was confirmed by DNA sequencing. Immunostaining against the Flag epitope tag inserted at the C-terminus of the T1R2 construct and against an antigenic peptide located the VFTM of T1R3 was performed on the transiently transfected HEK cells to control transfection efficiency of the mutants in comparison to wild type as described previously [37].

### Design of receptor mutants to test wedge models for brazzein-sweet receptor interaction

Several groups have hypothesized that brazzein and other protein sweeteners bind like a wedge within the open cleft of the sweet receptor's VFTMs: hence the name "wedge model" [22; 23; 25; 27; 28; 33]. Two alternative binding sites for brazzein on the sweet receptor have been proposed: within the open cleft of T1R2 VFTM [23] (Fig. 2A) or within the open cleft of T1R3 VFTM [28] (Fig. 2B). The wedge models suggest that residues within the open clefts as well as specific residues adjacent to the cleft in the opposite subunit are contact sites for sweet proteins (Fig. 2A and 2B) [23; 28]. These models imply a mechanism for signal transduction that is radically different from that postulated for other class C GPCRs, in which the cleft is in the closed conformation in the active state [14; 15; 50]. Therefore, we thought it was imperative to experimentally test these models by mutating residues at the proposed contact sites.

We mutated solvent-accessible residues in the clefts, along with several additional residues at the mouth of the cleft of each subunit (T1R2: E145, E170, R172, D173, Y215, R217 and T1R3: H145, E148, E172, Y218). The residues were mutated to alanine, and, in some cases, charged residues were mutated to the opposite charge. Mutant receptors were tested for responsiveness to brazzein, in comparison to a panel of other sweeteners: cyclamate, neotame (NTM), and sucralose. Two concentrations of brazzein were tested at 250 μg/ml (~$EC_{50}$) and 50 μg/ml (~threshold). Neotame (VFTM-T1R2 agonist) and cyclamate (TMs-T1R3 agonist) were used at sub-saturating concentrations (~5×$EC_{50}$) and served as sensor-controls for potential negative shifts in overall potency ($EC_{50}$) and efficacy (E) of the mutant receptors to sweeteners, in comparison to WT receptor.

### Heterologous calcium assay for sweet taste receptor

HEK293E cells were cultured at 37 °C in Optimum GlutaMAX culture medium (Invitrogen, Carlsbad, CA) supplemented with 4% dialyzed fetal bovine serum. Human T1R2 and T1R3 receptor clones were constructed as described previously [37]. The $G_{\alpha 16}$-gust44 onstruct was made according to established procedures [39]. Cells were transfected with the three constructs using Lipofectamine™2000 according to the manufacturer's protocol (Invitrogen, Carlsbad, CA). Cells were seeded onto 96-well poly-D-lysine plates (Corning) at about 12,500 cells/well 18 h prior to transfection; cells in each well were co-transfected with plasmid DNAs encoding T1Rs and $G_{\alpha 16}$-gust44 (0.1 μg total DNA/well; 0.2 μl Lipofectamine/well). After 24 h, the transfected cells were washed once with the culture medium. After an additional 24 h, the cells were washed once with HBSS supplemented with 20 mM HEPES, loaded with 3 μM Fluo-4AM (Molecular Probe) diluted in HBSS-HEPES buffer, incubated for 1.5 h at room temperature, and then washed with HBSS-HEPES and maintained in HBSS-HEPES at 25 °C. The plates of dye-loaded transfected cells were placed into a FlexStation II apparatus (Molecular Devices, Groton, CT) to monitor fluorescence (excitation, 488 nm; emission, 525 nm; cutoff, 515 nm).

Tastants were added 30 s after the start of the scan at 2× concentrations in 50 μl of HBSS-HEPES while monitoring fluorescence for an additional 200 s at 2 s intervals.

### Analysis of calcium responses

After obtaining a calcium mobilization trace for each sample, calcium responses to tastants were quantified as the percentage of the change (peak fluorescence - baseline fluorescence level, denoted as $\Delta F$) from the baseline fluorescence level (denoted as $F$); $\Delta F/F$. Peak fluorescence intensity occurred about 20–30 s after the addition of tastants. Typically, wild-type sweet receptors (T1R2+T1R3) along with $G_{\alpha 16}$-gust44 showed calcium signal increases of 40 to 100 % ($\Delta F/F$). Buffer alone evoked no significant response from transfected cells, and tastants evoked no significant responses from parental cells, cells transfected with disabled forms of the sweet receptor, or T1R3 alone ($3\ \% \leq \Delta F/F \leq 3\ \%$, S.E). The data were expressed as the mean ± SE of quadruplicate or sextuplicate of the $\Delta F/F$ values, or were normalized as described. Graph-Pad Prism 3.0 (GraphPad Software, Inc., San Diego, CA) software was used for curve fitting and creation of bar graphs.

### Structural model of T1R2/T1R3 VFTM and putative brazzein interacting residues

Homology-models (closed-open; open-closed) of the receptor extracellular parts of hT1R2 and hT1R3 heterodimer based on crystal structure of mGluR1 (PDB entry: 1ewk, 1ewt) were generated as described [20]. Figures were generated using Molsoft ICM software (La Jolla, CA). Residues selected for mutagenesis are represented by toggle sticks and whole VFTMs by mesh envelopes.

## Supplementary Material

Refer to Web version on PubMed Central for supplementary material.

## Acknowledgments

This research was supported by R01 DC009018, R01 DC006696, R01 DC008301, and R21 DC008805. NMR data were collected and analyzed at the National Magnetic Resonance Facility at Madison (NMRFAM). MM, JLM and FAP have personal financial interests as inventors on patents and patent applications which have been licensed to Redpoint Bio and Natur Research Ingredients. Inc.

## Abbreviations used

| | |
|---|---|
| brazzein | recombinant protein with sequence identical to the native protein lacking the N-terminal pyroglutamate (the numbering system used has Asp2 as the N-terminal residue) |
| hT1R2 | human T1R2 subunit of the sweet receptor (“h” is replaced with “m” to indicate mouse) |
| hT1R3 | human T1R3 subunit of the sweet receptor |
| VFTM | Venus fly trap module |
| CRD | cysteine rich domain |
| GPCR | G-protein coupled receptor |
| TMD | transmembrane domain |

## References


1. van der Wel H. Isolation and Characterization of the sweet principle from Dioscoreophyllum cumminsii (Stapf) Diels. FEBS Lett 1972;21:88–90. [PubMed: 11946482]
2. Morris JA, Cagan RH. Purification of monellin, the sweet principle of Dioscoreophyllum cumminsii. Biochimica et Biophysica Acta 1972;261:114–122. [PubMed: 5012458]
3. Nirasawa S, Nishino T, Katahira M, Uesugi S, Hu Z, Kurihara Y. Structures of Heat-Stable and Unstable Homologues of the Sweet Protein Mabinlin. European Journal of Biochemistry 1994;223:989–995. [PubMed: 8055976]
4. Ming D, Hellekant G. Brazzein, a New High-Potency Thermostable Sweet Protein from *Pentadiplandra brazzeana* B. FEBS Lett 1994;355:106–108. [PubMed: 7957951]
5. Izawa H, Ota M, Kohmura M, Ariyoshi Y. Synthesis and Characterization of the Sweet Protein Brazzein. Biopolymers 1996;39:95–101. [PubMed: 8924630]
6. Masuda T, Ueno Y, Kitabatake N. Sweetness and enzymatic activity of lysozyme. J Agric Food Chem 2001;49:4937–41. [PubMed: 11600047]
7. Nakajima K, Asakura T, Oike H, Morita Y, Shimizu-Ibuka A, Misaka T, Sorimachi H, Arai S, Abe K. Neoculin, a taste-modifying protein, is recognized by human sweet taste receptor. Neuroreport 2006;17:1241–4. [PubMed: 16951562]
8. Maehashi K, Matano M, Kondo A, Yamamoto Y, Udaka S. Riboflavin-binding protein exhibits selective sweet suppression toward protein sweeteners. Chem Senses 2007;32:183–90. [PubMed: 17167172]
9. van der Wel H, Larson G, Hladik A, Hellekant G, Glaser D. Isolation and Characterization of Pentadin, the Sweet Principle of *Pentadiplandra brazzeana* Baillon. Chemical Senses 1989;14:75–79.
10. Assadi-Porter FM, Aceti DJ, Cheng H, Markley JL. Efficient production of recombinant brazzein, a small, heat-stable, sweet-tasting protein of plant origin. Arch Biochem Biophys 2000;376:252–8. [PubMed: 10775410]
11. Assadi-Porter FM, Patry S, Markley JL. Efficient and rapid protein expression and purification of small high disulfide containing sweet protein brazzein in E. coli. Protein Expr Purif 2008;58:263–8. [PubMed: 18221889]
12. Caldwell JE, Abildgaard F, Dzakula Z, Ming D, Hellekant G, Markley JL. Solution structure of the thermostable sweet-tasting protein brazzein. Nat Struct Biol 1998;5:427–31. [PubMed: 9628478]
13. Nelson G, Hoon MA, Chandrashekar J, Zhang Y, Ryba NJ, Zuker CS. Mammalian sweet taste receptors. Cell 2001;106:381–390. [PubMed: 11509186]
14. Kunishima N, Shimada Y, Tsuji Y, Sato T, Yamamoto M, Kumasaka T, Nakanishi S, Jingami H, Morikawa K. Structural basis of glutamate recognition by a dimeric metabotropic glutamate receptor. Nature 2000;407:971–7. [PubMed: 11069170]
15. Muto T, Tsuchiya D, Morikawa K, Jingami H. Structures of the extracellular regions of the group II/III metabotropic glutamate receptors. Proc Natl Acad Sci U S A 2007;104:3759–64. [PubMed: 17360426]
16. Palczewski K, Kumasaka T, Hori T, Behnke CA, Motoshima H, Fox BA, Le Trong I, Teller DC, Okada T, Stenkamp RE, Yamamoto M, Miyano M. Crystal structure of rhodopsin: A G protein-coupled receptor. Science 2000;289:739–45. [PubMed: 10926528]
17. Pin JP, Kniazeff J, Binet V, Liu J, Maurel D, Galvez T, Duthey B, Havlickova M, Blahos J, Prezeau L, Rondard P. Activation mechanism of the heterodimeric GABA(B) receptor. Biochem Pharmacol 2004;68:1565–72. [PubMed: 15451400]
18. Xu H, Staszewski L, Tang H, Adler E, Zoller M, Li X. Different functional roles of T1R subunits in the heteromeric taste receptors. Proc Natl Acad Sci U S A 2004;101:14258–63. [PubMed: 15353592]
19. Brock C, Oueslati N, Soler S, Boudier L, Rondard P, Pin JP. Activation of a dimeric metabotropic glutamate receptor by intersubunit rearrangement. J Biol Chem 2007;282:33000–8. [PubMed: 17855348]
20. Cui M, Jiang P, Maillet E, Max M, Margolskee RF, Osman R. The heterodimeric sweet taste receptor has multiple potential ligand binding sites. Curr Pharm Des 2006;12:4591–600. [PubMed: 17168764]
21. Morini G, Bassoli A, Temussi PA. From small sweeteners to sweet proteins: anatomy of the binding sites of the human T1R2_T1R3 receptor. J Med Chem 2005;48:5520–9. [PubMed: 16107151]

22. Shimizu-Ibuka A, Morita Y, Terada T, Asakura T, Nakajima K, Iwata S, Misaka T, Sorimachi H, Arai S, Abe K. Crystal structure of neoculin: insights into its sweetness and taste-modifying activity. J Mol Biol 2006;359:148–58. [PubMed: 16616933]
23. Walters DE, Hellekant G. Interactions of the sweet protein brazzein with the sweet taste receptor. J Agric Food Chem 2006;54:10129–33. [PubMed: 17177550]
24. Jingami H, Nakanishi S, Morikawa K. Structure of the metabotropic glutamate receptor. Curr Opin Neurobiol 2003;13:271–8. [PubMed: 12850210]
25. Temussi PA. Natural sweet macromolecules: how sweet proteins work. Cell Mol Life Sci 2006;63:1876–88. [PubMed: 16810455]
26. Spadaccini R, Trabucco F, Saviano G, Picone D, Crescenzi O, Tancredi T, Temussi PA. The mechanism of interaction of sweet proteins with the T1R2-T1R3 receptor: evidence from the solution structure of G16A-MNEI. J Mol Biol 2003;328:683–92. [PubMed: 12706725]
27. Temussi PA. Why are sweet proteins sweet? Interaction of brazzein, monellin and thaumatin with the T1R2-T1R3 receptor. FEBS Lett 2002;526:1–4. [PubMed: 12208493]
28. Esposito V, Gallucci R, Picone D, Saviano G, Tancredi T, Temussi PA. The importance of electrostatic potential in the interaction of sweet proteins with the sweet taste receptor. J Mol Biol 2006;360:448–56. [PubMed: 16764888]
29. Igeta H, Tamura Y, Nakaya K, Nakamura Y, Kurihara Y. Determination of disulfide array and subunit structure of taste-modifying protein, miraculin. Biochim Biophys Acta 1991;1079:303–7. [PubMed: 1911854]
30. Kurimoto E, Suzuki M, Amemiya E, Yamaguchi Y, Nirasawa S, Shimba N, Xu N, Kashiwagi T, Kawai M, Suzuki E, Kato K. Curculin exhibits sweet-tasting and taste-modifying activities through its distinct molecular surfaces. J Biol Chem 2007;282:33252–6. [PubMed: 17895249]
31. Tancredi T, Iijima H, Saviano G, Amodeo P, Temussi PA. Structural determination of the active site of a sweet protein. A 1H NMR investigation of pMNEI. FEBS Lett 1992;310:27–30. [PubMed: 1526280]
32. Jiang P, Cui M, Ji Q, Snyder L, Liu Z, Benard L, Margolskee RF, Osman R, Max M. Molecular mechanisms of sweet receptor function. Chem Senses 2005;30(Suppl 1):i17–i18. [PubMed: 15738096]
33. Koizumi A, Nakajima K, Asakura T, Morita Y, Ito K, Shmizu-Ibuka A, Misaka T, Abe K. Taste-modifying sweet protein, neoculin, is received at human T1R3 amino terminal domain. Biochem Biophys Res Commun 2007;358:585–9. [PubMed: 17499612]
34. Assadi-Porter FM, Aceti DJ, Markley JL. Sweetness determinant sites of brazzein, a small, heat-stable, sweet-tasting protein. Arch Biochem Biophys 2000;376:259–65. [PubMed: 10775411]
35. Jin Z, Danilova V, Assadi-Porter FM, Aceti DJ, Markley JL, Hellekant G. Critical regions for the sweetness of brazzein. FEBS Lett 2003;544:33–7. [PubMed: 12782286]
36. Jin Z, Danilova V, Assadi-Porter FM, Markley JL, Hellekant G. Monkey electrophysiological and human psychophysical responses to mutants of the sweet protein brazzein: delineating brazzein sweetness. Chem Senses 2003;28:491–8. [PubMed: 12907586]
37. Jiang P, Ji Q, Liu Z, Snyder LA, Benard LM, Margolskee RF, Max M. The cysteine-rich region of T1R3 determines responses to intensely sweet proteins. J Biol Chem 2004;279:45068–75. [PubMed: 15299024]
38. Green BG, Dalton P, Cowart B, Shaffer G, Rankin K, Higgins J. Evaluating the 'Labeled Magnitude Scale' for measuring sensations of taste and smell. Chemical Senses 1996;21:323–34. [PubMed: 8670711]
39. Ueda T, Ugawa S, Yamamura H, Imaizumi Y, Shimada S. Functional interaction between T2R taste receptors and G-protein alpha subunits expressed in taste receptor cells. J Neurosci 2003;23:7376–80. [PubMed: 12917372]
40. Sharma D, Rajarathnam K. $^{13}$C NMR chemical shifts can predict disulfide bond formation. Journal of Biomolecular NMR 2000;18:165–171. [PubMed: 11101221]
41. Jiang P, Cui M, Zhao B, Liu Z, Snyder LA, Benard LM, Osman R, Margolskee RF, Max M. Lactisole interacts with the transmembrane domains of human T1R3 to inhibit sweet taste. J Biol Chem 2005;280:15238–46. [PubMed: 15668251]

42. Assadi-Porter FM, Abildgaard F, Blad H, Markley JL. Correlation of the sweetness of variants of the protein brazzein with patterns of hydrogen bonds detected by NMR spectroscopy. J Biol Chem 2003;278:31331–9. [PubMed: 12732626]
43. Assadi-Porter FM, Abildgaard F, Blad H, Cornilescu CC, Markley JL. Brazzein, a small, sweet protein: effects of mutations on its structure, dynamics and functional properties. Chem Senses 2005;30 (Suppl 1):i90–i91. [PubMed: 15738211]
44. Assadi-Porter, FM.; Tonelli, M.; Markley, JL. Correlation of sweetness to structure and dynamics properties in brazzein protein analogs. In: Dubois, DKWaGE., editor. Sweetness and Sweeteners: Biology, Chemistry and Psychophysics. Vol. 979. Oxford University Press; 2008. p. 560-572.
45. Tancredi T, Pastore A, Salvadori S, Esposito V, Temussi PA. Interaction of sweet proteins with their receptor. A conformational study of peptides corresponding to loops of brazzein, monellin and thaumatin. Eur J Biochem 2004;271:2231–40. [PubMed: 15153113]
46. Assadi-Porter FM, Tonelli M, Maillet EL, Markley JL, Max M. Interactions between the human sweet-sensing T1R2-T1R3 receptor and sweeteners detected by saturation transfer difference NMR spectroscopy. Biochim Biophys Acta. 2009
47. Nie Y, Vigues S, Hobbs JR, Conn GL, Munger SD. Distinct contributions of T1R2 and T1R3 taste receptor subunits to the detection of sweet stimuli. Curr Biol 2005;15:1948–52. [PubMed: 16271873]
48. Tsuchiya D, Kunishima N, Kamiya N, Jingami H, Morikawa K. Structural views of the ligand-binding cores of a metabotropic glutamate receptor complexed with an antagonist and both glutamate and Gd3+ Proc Natl Acad Sci U S A 2002;99:2660–5. [PubMed: 11867751]
49. Scopes RK. Measurement of protein by spectrophotometry at 205 nm. Anal Biochem 1974;59:277–82. [PubMed: 4407487]
50. Kniazeff J, Bessis AS, Maurel D, Ansanay H, Prezeau L, Pin JP. Closed state of both binding domains of homodimeric mGlu receptors is required for full activity. Nat Struct Mol Biol 2004;11:706–13. [PubMed: 15235591]

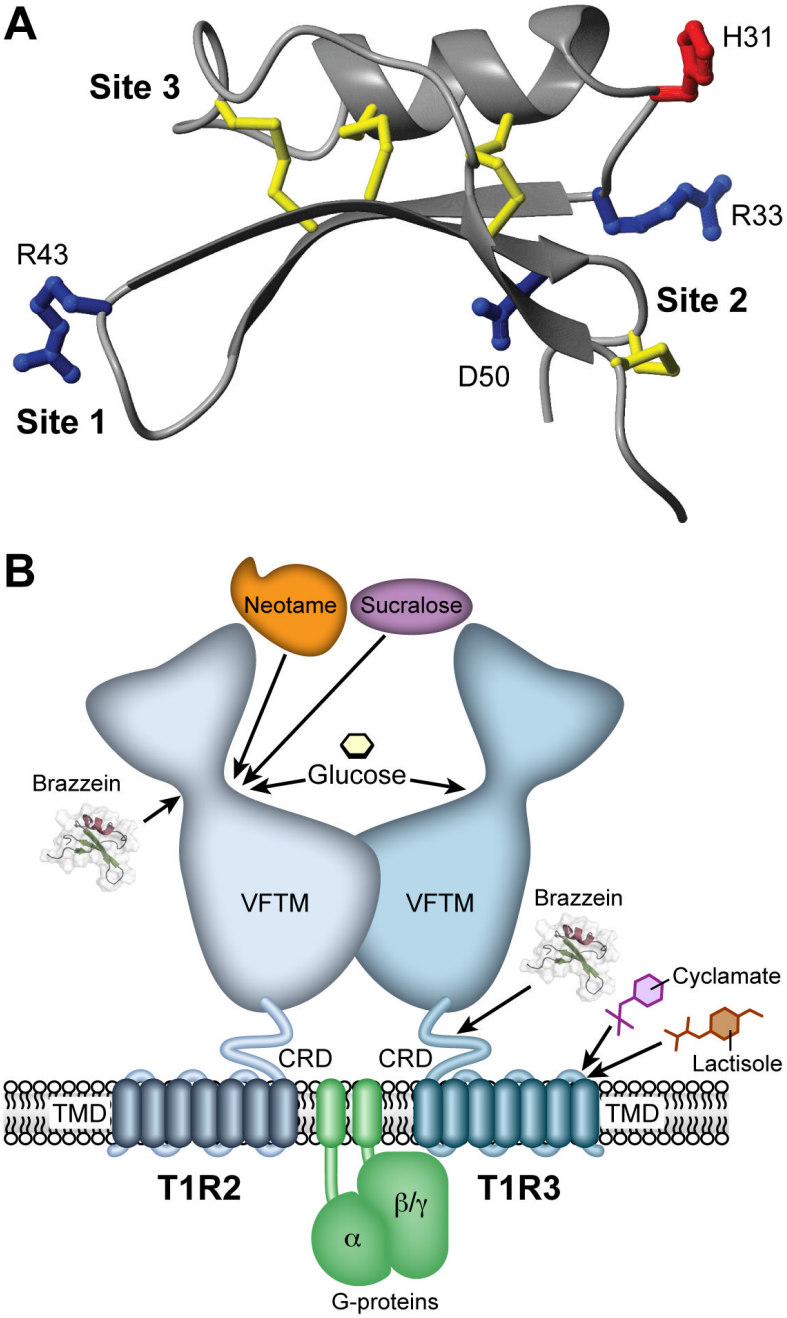


**Figure 1.**

**A.** Backbone structure of brazzein showing the three "sweet sites" determined previously [36]. The numbering system used is that for the wild-type variant that does not contain pGlu1 and has Asp2 as the N-terminal residue. **B.** Schematic representation of the GPCR sweet sensor T1R2-T1R3 heterodimer: VFTM, the extracellular Venus fly trap module; CRD, the extracellular cysteine-rich domain; TMD, the 7 transmembrane α-helices; C-term, the C-terminal intracellular tail. Arrows represent binding locations proposed for several ligands: the sweeteners alitame, D-trp (VFTM of T1R2) and cyclamate (TMD of T1R3), the anti-sweet agent lactisol (TMD of T1R3), whereas brazzein binding locations are to VFTM of T1R2 and CRD of T1R3.

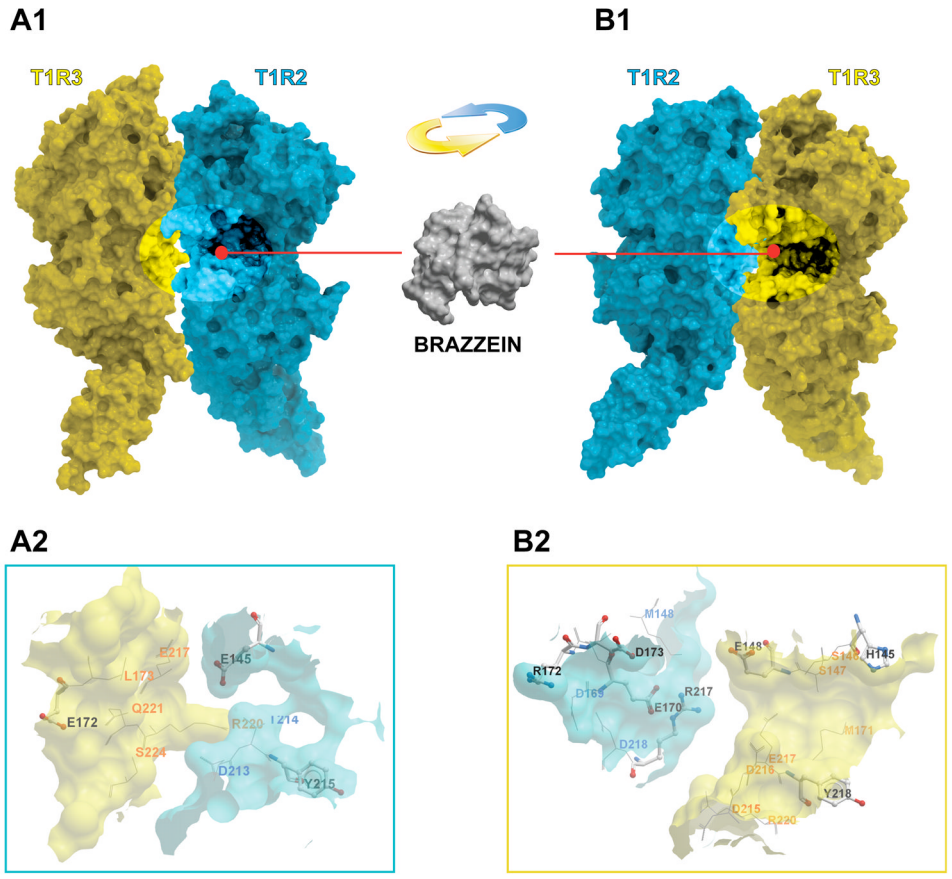


**Figure 2.**

Wedge models of interactions between the sweet receptor and sweet proteins. Homology-modeled structures of the Venus fly trap modules of T1R2 and T1R3, with the Cysteine-rich domains (CRD). T1R2 is shown in blue; T1R3 is shown in yellow. **(Top panels) A1.** T1R3-closed/T1R2-open, **B1.** T1R2-closed/T1R3-open. Brazzein (grey) has been predicted to fit in the cavity of the mouth of the VFTM of either T1R2 (**A**) or T1R3 (**B**), and to contact interface proximal residues from the other subunit. The binding surface of the receptor to brazzein predicted by the wedge models [23; 25; 26; 28] are represented as a mesh envelope with highlighted surfaces. An expanded view of this region is represented in the bottom panels**. (Bottom panels) A2.** Ball-and-stick representation of the residues that might be involved in brazzein binding when fitted in the open-VFTM cleft of T1R2: T1R3-E172; T1R2:E145,Y215. **B2.** Ball-and-stick of the residues that might be involved in brazzein binding when fitted in the open-VFTM cleft of T1R3: T1R2:E170,R172,D173,R217; T1R3:E148,H145,Y218. Stick representation of other potentially interacting residues are also displayed in **A2** and **B2**.

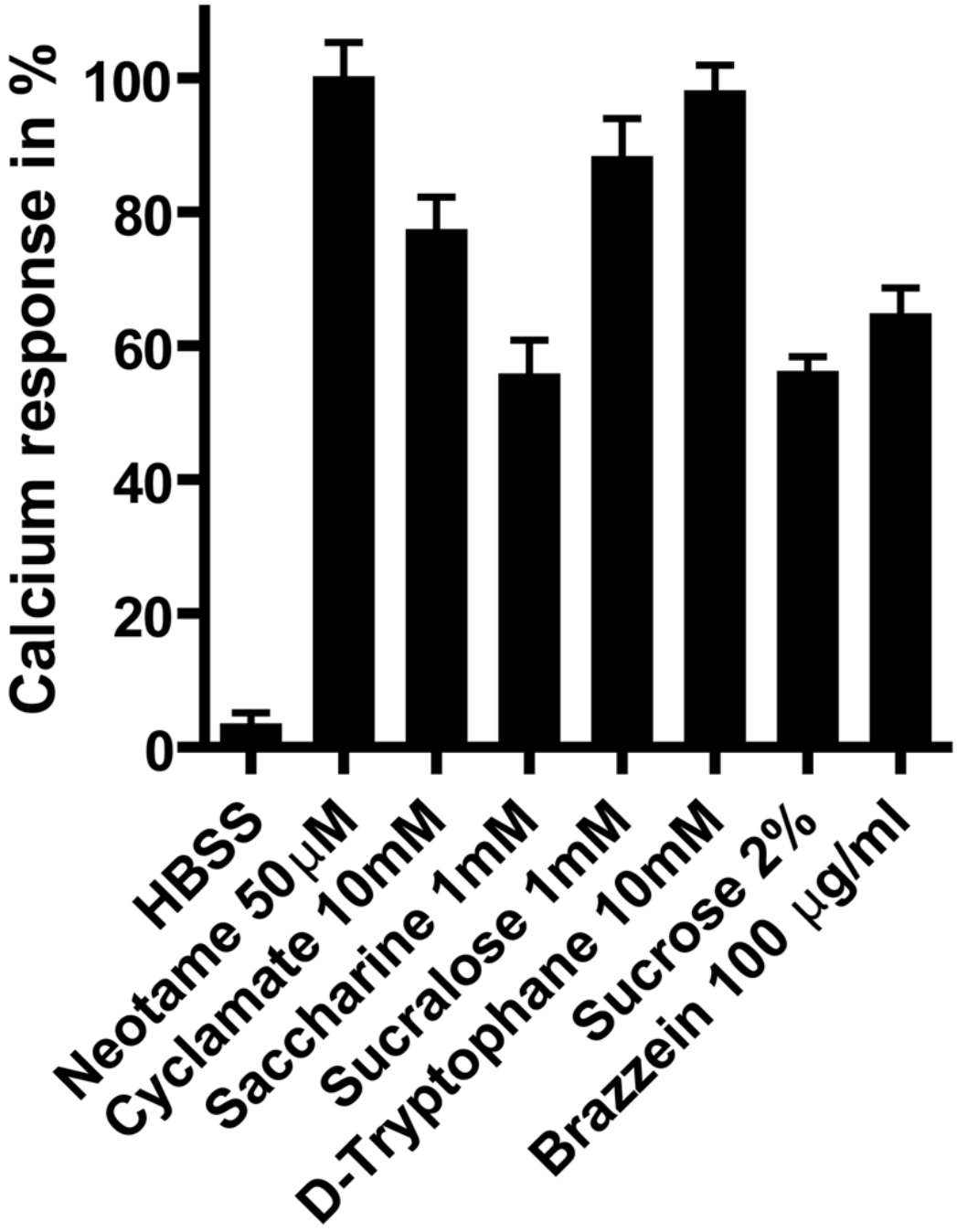


**Figure 3.**

Profile of the responses of the heterologously expressed human sweet receptor to a panel of sweeteners by the calcium mobilization assay. Human T1R2 and human T1R3 heterodimer sweet taste receptors were expressed in HEK293 cells along with the promiscuous G-protein chimera G16-gus44. Activity of the human sweet receptor in response to sweeteners was quantified by calcium imaging: all sweeteners, except sucrose and brazzein, were at saturating concentrations. HBSS buffer (used as dilution buffer for sweeteners) provides a negative control for sweet responses. Calcium mobilization is quantified as the peak of fluorescence response over baseline ($\Delta F/F$) and normalized to the response of neotame. Data are mean ± SE of a single representative experiment.

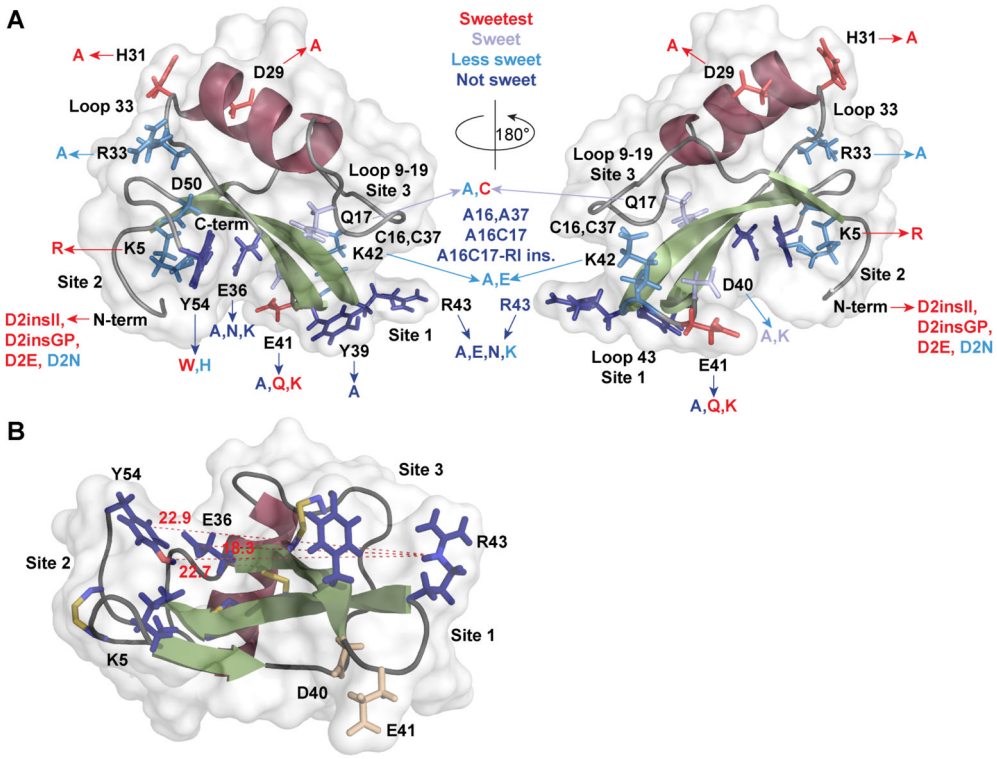


**Figure 4.**

**A.** Surface representation (left side “front” view; right side “back” view) of wild type brazzein showing the positions of mutations found to affect sweetness. Mutations that abolished sweetness are shown in dark blue; those that profoundly decreased sweetness relative to wild type are in medium blue; those that slightly decreased sweetness are in light blue; those that enhanced sweetness are in red. **B.** Location of the three “sweet sites”: Site 1 (Loop43), Site 2 (N- and C-termini, E36), and Site 3 (Loop9–19). The three sites form a non-continuous surface that spans about 18–20 Å [34; 35].

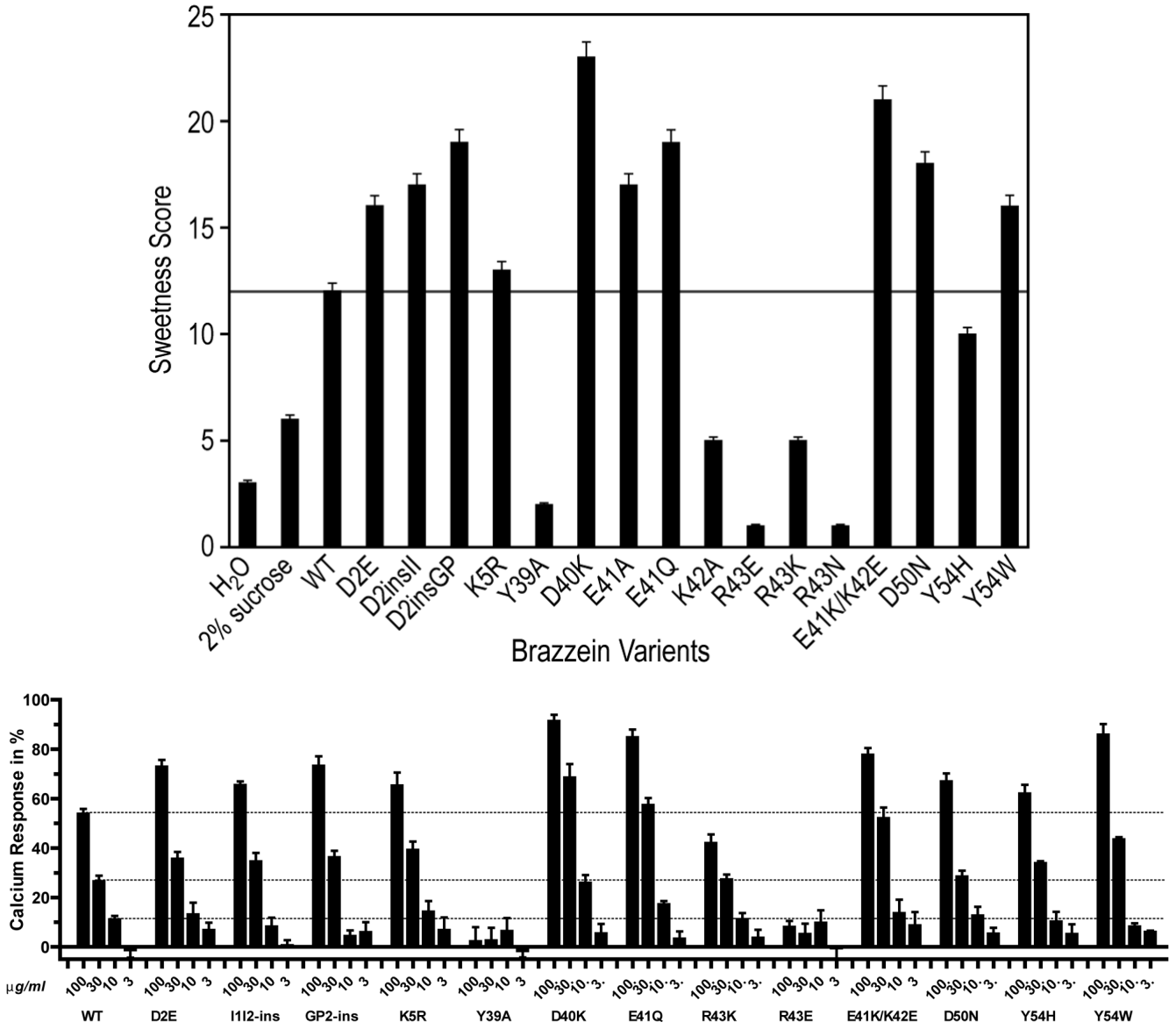


**Figure 5.**

**A**. Psychophysical analysis (taste panel) of wild type brazzein (WT) and a series of brazzein mutants. The study used brazzein protein concentrations of 100 μg/ml in comparison to a 2% solution of sucrose. Results from 10 subjects were averaged. The Y-axis indicates the sweetness score for wild type brazzein and its mutants in comparison with sucrose. Error bars represent mean ± SE. **B.** Activity of wild type brazzein and its mutants assayed by heterologous expression of the human sweet receptor (T1R2+T1R3) assayed by calcium mobilization in the presence of a reporter G-protein (G16-gus44). The calcium assay was carried out at four concentrations of wild type or mutant brazzeins: 100, 30, 10, and 3 μg/ml. The maximal response of the receptors in each experiment was quantified using a saturation concentration of the agonist neotame (50μM), and data were normalized to 100 % of this value. Values represent mean ± S.E of three independent experiments.

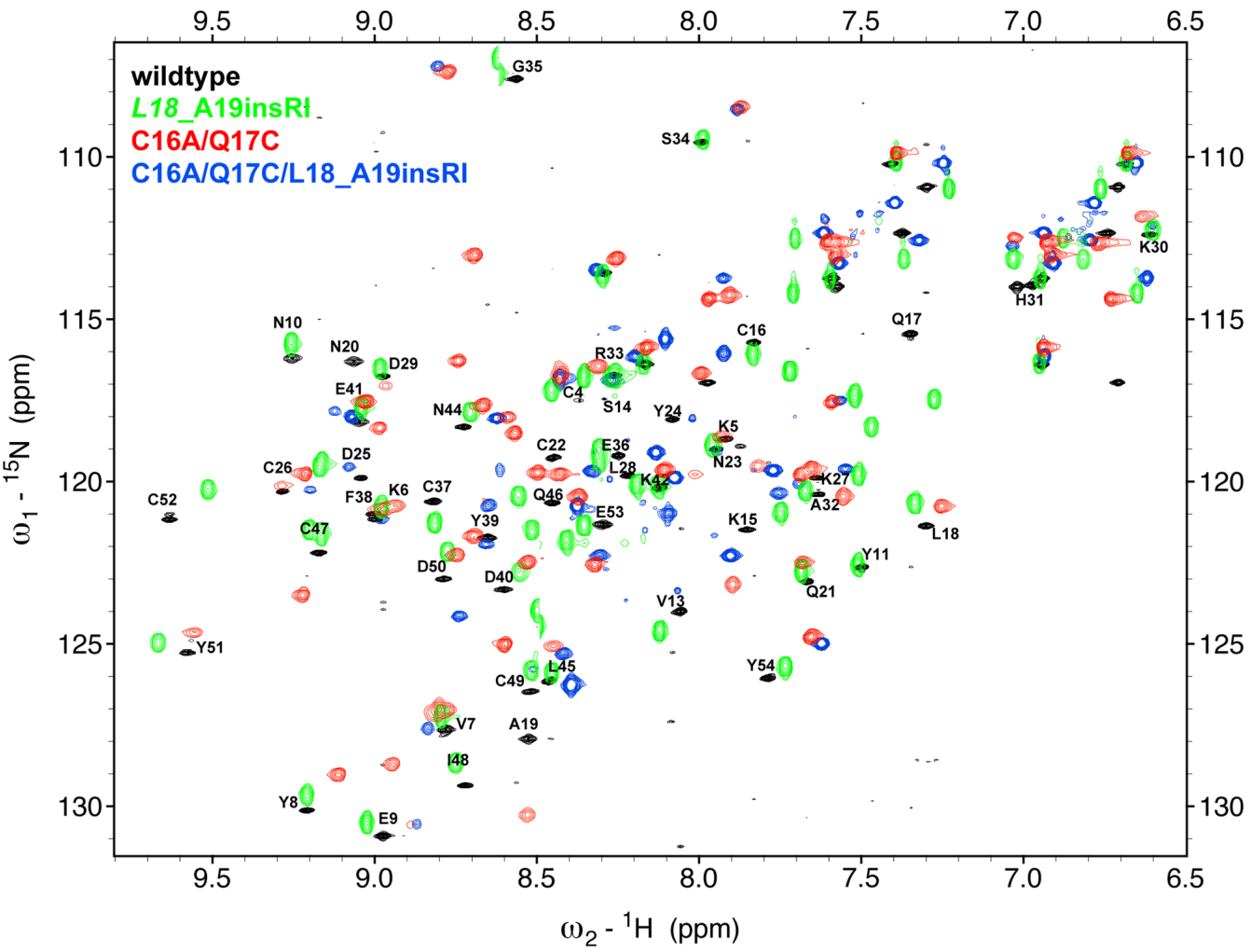


**Figure 6.**

Overlay of heteronuclear $^{15}$N-$^{1}$H HSQC spectra (fingerprint amide region) of wild type brazzein (black) and three “non-sweet” brazzein variants: L18_A19insRI ns (green), C16A/Q17C (red), C16A/C37A (blue). Psychophysical testing demonstrated that mutant L18_A19insRI, which contains two residues RI inserted between L18 and A19 of wild type brazzein, is tasteless. NMR chemical shift mapping of differences between this mutant and brazzein indicated that the residues affected by the insertion are localized to the mutated loop and to the region of the single $\alpha$-helix.

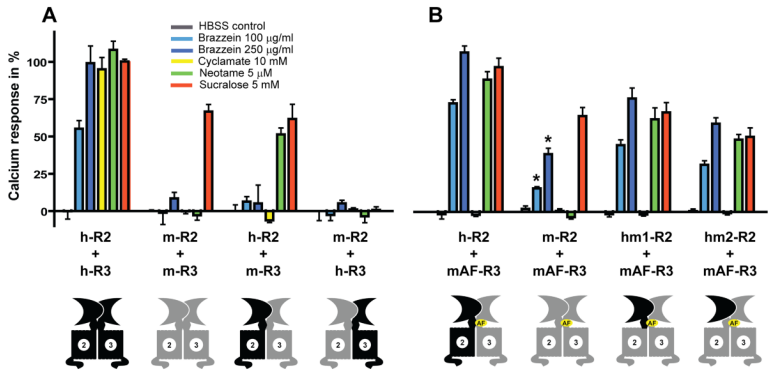


**Figure 7.**

The human T1R2 extracellular domain Venus-FlyTrap Module determines sensitivity to brazzein. Human (hT1R2+hT1R3), mouse (mT1R2+mT1R3) and chimeric mouse/human sweet receptors (as indicated by m/h prefix) and brazzein-permissible mouse T1R3 mutant T542A/P545F (mAF-R3) were activated by brazzein, cyclamate, neotame and sucralose and assayed for calcium responses. Chimeric receptors of T1R2 contained the extracellular portion (VFTM and CRD as for hm1-R2, or VFTM alone as for hm2-R2) of human receptor, and the CRD and/or only the transmembrane domain and C-terminal from mouse; as shown in the black/grey schematics receptor. Peak calcium signal is expressed as $\Delta F/F$ in %, normalized to maximal response to sucralose (5mM= ~25 $EC_{50}$). Data in the figure are from a representative experiment, means ± SE, done in quadruplicate. The star * represents P<0.001 difference of mT1R2 in comparison to the sweetener profile of hT1R2, when paired with mAF-T1R3.

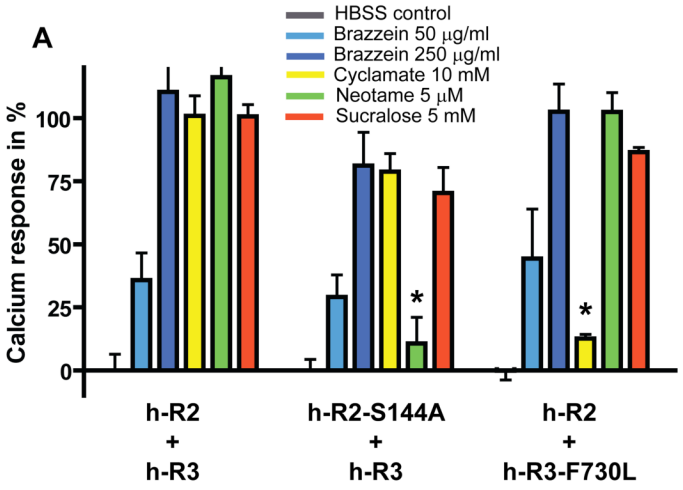


B

| T1R2 | T1R3 | Brazzein 50μg/ml | Brazzein 250μg/ml | Cyclamate 10mM | Neotame 5μM | Sucralose 5mM |
|---|---|---|---|---|---|---|
| WT | WT | ++ | +++++ | +++++ | +++++ | +++++ |
| S144A[a] | WT | ++ | ++++ | ++++ | + | ++++ |
| WT | F730L[b] | ++ | +++++ | + | +++++ | ++++ |

C

| T1R2 | T1R3 | Brazzein 50μg/ml | Brazzein 250μg/ml | Cyclamate 10mM | Neotame 5μM | Sucralose 5mM |
|---|---|---|---|---|---|---|
| WT | WT | ++ | +++++ | +++++ | +++++ | +++++ |
| E145A | WT | + | ++++ | ++++ | ++++ | ++++ |
| E145R | WT | + | ++ | ++ | ++ | ++ |
| Y215A | WT | - | - | - | - | - |
| WT | E172A | + | +++ | ++ | ++ | +++ |
| WT | E172R | - | + | + | - | + |

D

| T1R2 | T1R3 | Brazzein 50μg/ml | Brazzein 250μg/ml | Cyclamate 10mM | Neotame 5μM | Sucralose 5mM |
|---|---|---|---|---|---|---|
| WT | WT | ++ | +++++ | +++++ | +++++ | +++++ |
| E170K | WT | ++ | +++ | +++ | +++ | +++ |
| R172A | WT | + | +++ | ++++ | ++ | +++ |
| R172D | WT | - | + | + | + | + |
| D173A | WT | - | + | - | - | - |
| D173R | WT | - | + | - | - | + |
| R217A | WT | - | ++ | +++ | ++ | +++ |
| R217D | WT | - | - | - | - | - |
| WT | H145A | ++ | ++++ | ++++ | ++++ | +++++ |
| WT | E148A | + | +++ | +++ | ++ | ++ |
| WT | E148R | ++ | +++++ | ++++ | ++++ | ++++ |
| WT | Y218A | - | - | - | - | - |

**Figure 8.**

Receptor mutants designed to test putative interaction sites in wedge models. WT and mutant receptor responses to two non-saturating concentrations of brazzein (50 and 250 μg/ml), sub-saturating concentrations of neotame (5 μM) and cyclamate (10 mM) and saturating concentration of sucralose (5 mM) were assayed by calcium mobilization. Peak calcium signal is expressed as Δ*F*/*F* in %, normalized to control (WT with sucralose). Values are means ± SE from at least three independent experiments. The star "*" represents P<0.001 difference of mutant receptors in comparison to WT sweetener profile. **(Tables).** Each "+" represents an increment of % of calcium response. "–":≤ 10%. "+":10><25. "++":25><50. "+++":50><75. "++++":75><100. "+++++":≥100. **A** and **B.** Neotame is a VFTM-T1R2 binding ligand and

cyclamate is a TM-T1R3 binding ligand. Mutants T1R2-S144A[a] [18], and T1R3-F730L[b] [41], have been shown to specifically affect neotame and cyclamate response respectively. **C and D.** Mutants were chosen on the basis of the putative binding site(s) for brazzein shown in Figure 2. **C.** Residues that might be involved in brazzein binding when fitted in the open-VFTM cleft of T1R2: T1R3-E172; T1R2:E145,Y215. **D.** Residues that might be involved in brazzein binding when fitted in the open-VFTM cleft of T1R3: T1R2:E170,R172,D173,R217; T1R3:E148,H145,Y218.

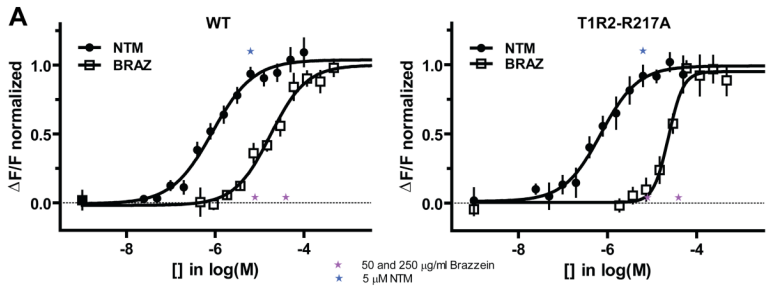


**B**

| | WT | | T1R2-R217A | |
|---|---|---|---|---|
| | EC50 | $n_{HILL}$ | EC50 | $n_{HILL}$ |
| Neotame | 8.3 ± 2.5e-07 | 1.37 ± 0.04 | 6.7 ± 1.9e-07 | 1.38 ± 0.33 |
| Cyclamate | 1.9 ± 0.8 e-03 | 1.27 ± 0.17 | 6.3 ± 1.7e-04 | 1.20 ± 0.16 |
| Sucralose | 6.5 ± 2.0e-05 | 1.46 ± 0.39 | 12 ± 3.1e-05 | 2.51 ± 0.19 |
| Brazzein | 1.6 ± 0.5e-05 | 1.20 ± 0.19 | 2.4 ± 0.6e-05 | 2.35 ± 0.74 |
| Monellin | 1.1 ± 0.2e-05 | 1.37 ± 0.07 | 1.4 ± 0.4e-05 | 2.93 ± 0.59 |

**Figure 9. The effect of receptor mutant T1R2:R217A on responses to the panel of sweeteners**

**A**. Dose-response analysis of neotame-activated (NTM) and brazzein-activated (braz) human receptor T1R2 + T1R3 and T1R2:R217A + T1R3. Peak calcium signal is expressed as $\Delta F/F$, normalized to saturation. Data are merged from several experiments; data-points are means ± SD. Stars mark the positions of 50 and 250μg brazzein in order to facilitate comparisons to the responses of R217A in Sup. Fig. 1. **B**. $EC_{50}$ values and slope values ($n_{HILL}$) of the dose-responses curves to neotame, cyclamate, sucralose, brazzein and monellin for WT and T1R2:R217A mutant. Values are means ± SE from at least three independent experiments.

## Table 1

Summary of new brazzein mutations investigated here, their location in the three sweet sites, and their effect on sweetness.

| Type of mutation | Location of the mutation (effect on sweetness) [1] | | |
|---|---|---|---|
| | **Site 1 Loop43** | **Site 2 N- and C-termini/residue 36** | **Site 3 Loop9–19** |
| Larger residue changed to Ala | Y39A (−−−)<br>E41A (++)<br>K42A (−−) | | |
| Change of side chain size | R43K (−−) | Y54H (−)<br>Y54W (+)<br>K5R (nc)<br>D2 (+) | D2E (+) |
| Negative to positive | D40K (+++) | | |
| Positive to negative | R43E (−−−) | | |
| Charge swap | E41K/K42E (+++) | | |
| Charge to neutral | E41Q (++)<br>R43N (−−−) | D50N (++) | |
| Insertions | | D2insII (+)<br>D2insGP (+) | L18_A19insRI (ns) |
| Disulfide removal | | | C16A/C37A (ns) |
| Disulfide move | | | C16Q17-A16C17 (ns) |
| Insertion and disulfide move | | | C16A/Q17C/L18_A19insRI (ns) |

[1] Key: nc, – no change; ns, completely non sweet; −− greatly reduced sweetness; −−−, profoundly reduced sweetness; +, mildly increased sweetness; ++, greatly increased sweetness; +++, maximally increased sweetness.

## Table 2

Summary of sweet receptor mutations and chimera investigated here, their location, and their effect on the response in the calcium flux assay.

| T1R2 | T1R3 | Response in the calcium flux assay |
|---|---|---|
| hT1R2 | hT1R3 | Robust, wild-type response (Fig. 8B,C,D) |
| mT1R2 | mT1R3 | No response to brazzein |
| hT1R2 | mT1R3 | No response to brazzein |
| mT1R2 | hT1R3 | No response to any sweetener tested |
| hT1R2 | mT1R3:T542A/P545F | Robust brazzein response, wild-type |
| mT1R2 | mT1R3:T542A/P545F | Less robust brazzein response |
| mT1R2:hVFTM/hCRD | mT1R3:T542A/P545F | Robust, wild-type |
| mT1R2:hVFTM | mT1R3:T542A/P545F | Robust, wild-type |
| hT1R2:S144A | hT1R3 | Specific decrease in sensitivity to neotame (Fig. 8B) |
| hT1R2:E145A | hT1R3 | (Fig. 8C) |
| hT1R2:E145R | hT1R3 | (Fig. 8C) |
| hT1R2:E170K | hT1R3 | (Fig. 8D) |
| hT1R2:R172A | hT1R3 | (Fig. 8D) |
| hT1R2:R172D | hT1R3 | (Fig. 8D) |
| hT1R2:D173A | hT1R3 | No response to any sweetener tested (Fig. 8D) |
| hT1R2:D173R | hT1R3 | No response to any sweetener tested (Fig. 8D) |
| hT1R2:Y215A | hT1R3 | No response to any sweetener tested (Fig. 8C) |
| hT1R2:R217A | hT1R3 | Selective decrease in response to brazzein in comparison to other sweeteners; maximal response to neotame, cyclamate, sucralose, brazzein, and monellin half that of WT; $n_{Hill}$ for brazzein, monellin, and sucralose higher than for WT (Fig. 8D, 9) |
| hT1R2:R217D | hT1R3 | No response to any sweetener tested (Fig. 8D) |
| hT1R2 | hT1R3:H145A | (Fig. 8D) |
| hT1R2 | hT1R3:E148A | (Fig. 8D) |
| hT1R2 | hT1R3:E148R | (Fig. 8D) |
| hT1R2 | hT1R3:R172A | (Fig. 8C) |
| hT1R2 | hT1R3:E172R | No response to any sweetener tested (Fig. 8C) |
| hT1R2 | hT1R3:Y218A | No response to any sweetener tested (Fig. 8D) |
| hT1R2 | hT1R3:Y218R | No response to any sweetener tested |
| hT1R2 | hT1R3:F730L | Specific decrease in sensitivity to cyclamate (Fig. 8B) |